J Electroceram (2008) 21:193–197
DOI 10.1007/s10832-007-9107-5

Comparing macroscopic and microscopic properties of seeded ferroelectric thin films

Aiying Wu · G. Gonzalez-Aguilar · P. M. Vilarinho · I. M. Miranda Salvado · M. E. V. Costa

Published online: 7 April 2007

Abstract The comparison of macroscopic and microscopic properties of ferroelectric thin films in the systems of lead zirconate titanate (PZT) and strontium bismuth tantalate (SBT) with and without seeds is carried out. Microscopic properties were studied by piezo-response force microscopy (PFM). The local piezoelectric properties with and without seeds are compared with their macroscopic electric properties measured by conventional techniques. Previous microstructure analysis of PZT thin films showed that an intermetallic Pt_xPb layer between PZT and Pt, formed during the annealing process, was reduced and even eliminated in seeded PZT films. In SBT films, the addition of SBT seeds suppressed the interdiffusion of Pt and film components. Hence, the interfaces of PZT/substrate and SBT/substrate are modified by the presence of seeds, and their electrical properties are improved. In both PZT and SBT films, the remanent polarization values are higher in seeded films than in unseeded ones. Similarly, local piezo-response signal of single grain showed higher longitudinal piezoelectric coefficient d_{33} in seeded films than in unseeded ones. The critical voltage in which the ferroelectric domain starts to switch is lower in seeded films than in unseeded ones. The analysis of nanoscale switching in PZT and SBT films by PFM is presented and related to the corresponding macroscopic electric properties.

Keywords Ferroelectric thin films · Seeding · Local piezoelectric properties · PZT · SBT

A. Wu (✉) · G. Gonzalez-Aguilar · P. M. Vilarinho · I. M. Miranda Salvado · M. E. V. Costa
Department of Ceramic & Glass Engineering, CICECO, University of Aveiro,
3810 Aveiro, Portugal
e-mail: aiying@cv.ua.pt

1 Introduction

In the past 20 years, perovskite thin film have attracted much attention due to their applicability to dynamic random access memory (DRAM) and ferroelectric random access memory (FRAM) [1, 2]. Their high speed, nonvolatility, and light weight, combined with low power requirements, physical robustness, and high density, suggested that they would rapidly replace core memories as the nonvolatile memory for most applications. Because in single-crystal or bulk ceramics the operating voltages are too high to permit devices to be compatible with standard silicon integrated circuit logic levels (5.0±0.5 V for CMOS-TTL), thin films have been receiving considerable attentions. Among several materials, PZT ($PbZr_xTi_{1-x}O_3$), and more recently, bi-layered compounds are the most attractive candidates for memories and logic devices, and in the thin film form they meet the requirements of low-drive voltage, optimization of storage density, and switching transients. Compared with PZT, SBT ($SrBi_2Ta_2O_9$) also have been attracting because it exhibits little fatigue even after 10^{12} times polarization reversals.

Modern electronic industry requires the integration of different functional thin films into different structures in the device. Hence, the temperature of post-deposition treatment required for the crystallization of the functional oxides is a key parameter in the preparation of ferroelectric films. It ensures phase purity and controls interdiffusion between the film and underlayers, which have a direct impact on the film properties. Low processing temperatures are crucial to minimize the interdiffusion between different layers, undesired chemical reactions, and thermal degradation of the underlying circuit. As a consequence, the reliability of the devices will increase.

A new methodology that involved the utilization of diphasic precursor in which nanoparticles (seeds) are dispersed, has been used to decrease the crystallization temperature of some ferroelectric thin films [3]. More recently, the modification of the microstructural and electrical properties of ferroelectric thin films prepared via this methodology have been reported [4–6]. The overall activation energy for the perovskite crystallization was reduced, and the pure crystalline phase was obtained at low temperatures [7]. The microstructure of the film was optimized and the interfacial reaction minimized. Using nanoseeds in chemical solution deposition (CSD) precursors, the macroscopic electric properties of ferroelectric films of PZT and SBT have been improved. However, the mechanism of the modification of electric properties is not completely understood. For that, the relation between the local and macroscopic electric properties will be an added value. This work analyzes the local electric properties of two ferroelectric systems: PZT and SBT. The microscopic characterization of PZT and SBT thin films prepared by diphasic precursor was done by piezo-response force microscopy (PFM). The local piezoelectric properties of the films with and without seeds are compared and discussed. Meanwhile, these microscopic properties are compared with their macroscopic electric properties measured by conventional techniques.

2 Experimental

For preparing PZT thin films, a 0.4 M PZT precursor sol, with the ratio of Pb:Zr:Ti 1:0.52:0.48, was prepared using $[(CH_3CO_2)_2–Pb·3H_2O]$, $Zr[n\text{-}OCH(CH_3)_2]_4$ and $Ti[i\text{-}OCH(CH_3)_2]_4$ as reagents, and the details were in literature [4]. PZT(52/48) seeds (20–80 nm) were prepared by a sol–gel process described in Wu et al. [4]. Seeded PZT sols (5 wt% seeds) were prepared by mixing PZT seeds and the PZT precursor sol with the help of an ultrasonic probe. The substrates were platinized Si monocrystal ($Pt/Ti/SiO_2/Si$). Just before the deposition, the suspension was sonicated for 20 min. PZT(52/48) films were prepared by dip-coating using a withdrawal speed of 1.7 mm/s. The gel films were pyrolized at 300 °C for 1 min. This procedure was repeated four times to achieve a final film thickness of ~300 nm. Films were finally annealed at 550 °C for 30 min by directly inserting the sample into the furnace.

For preparing SBT thin films, $Bi(CH_3CO_2)_3$ was dissolved in a mixture (1:1) of toluene and acrylic acid hereafter described as TAc mixture. Then, $Sr(CH_3CO_2)_2$ was added, forming a clear solution. This solution was mixed with $Ta(OC_2H_5)_5$ under controlled atmosphere. This precursor was used for the deposition of films. SBT seed preparation was described elsewhere [6]. A seeded suspension was obtained by adding an appropriate amount of SBT seeds to a TAc mixture under ultrasonic stirring. The suspension was settled for 30 min, and the supernatant suspension (approximately 5 wt% solid content) was then used for seeding purposes. In preparing a seeded substrate, several drops of the seed suspension were deposited by spin-coating on a $Pt/Ti/SiO_2/Si$ substrate and subsequently dried at 130 °C. The seeded and unseeded films were prepared by spin-coating the precursor solution on seeded and unseeded $Pt/Ti/SiO_2/Si$ substrates at 3,000 rpm for 30 s. Then, the films were pyrolized at 325 °C and the spinning–drying–pyrolisis cycle was repeated until reaching the desired film thickness of 300 nm. Finally, the films were annealed in a tube furnace at 720 °C for 20 min in air.

The thickness and microstructure of the films were characterized by scanning electron microscopy (SEM), energy dispersive x-ray spectroscopy (EDS), and x-ray diffraction (XRD). Dielectric hysteresis loops were acquired using a thin film analyzer (TFA). Local piezoelectric properties of the films were analyzed via PFM that relies on a local piezoelectric effect exhibited by the film's surface. A commercial atomic force microscope (AFM) (Nanoscope IIIA) was used in the experiment with conductive Pt-coated Si tip-cantilevers (NSG01/Pt, NT-MDT) as top electrodes and for vibration detection. The ferroelectric film was excited by an external ac voltage applied between the PFM tip and the bottom electrode, and the deflection signal from the cantilever was detected by a lock-in amplifier. A topographic image of the film surface was taken simultaneously with the domain imaging.

3 Results and discussion

A marked improvement on the perovskite phase formation was observed when PZT or SBT seeds were added, indicating a faster phase transformation. XRD pattern of seeded PZT films annealed at 550 °C [inset of Fig. 1(a)] exhibit the pure perovskite phase, in contrast with unseeded films, in which the pyrochlore phase is still presented. The XRD patterns of SBT films, seeded and unseeded, prepared at 720 °C are ascribed to both fluorite and perovskite phases [inset of Fig. 1(b)]. Perovskite coexists with fluorite in the unseeded films but becomes dominant in seeded ones.

PZT and SBT seeds distributed in the films act as preferential nucleation sites, and the perovskite phase formation is promoted at lower temperatures as well, attested by XRD patterns of seeded films.

The PZT peak intensity was clearly enhanced in the case of seeded films. Crystallization kinetic studies of PZT(52/48) seeded and unseeded films [7] showed that the overall activation energy was reduced from 219 kJ/mol (unseeded) to 146 kJ/mol (seeded).

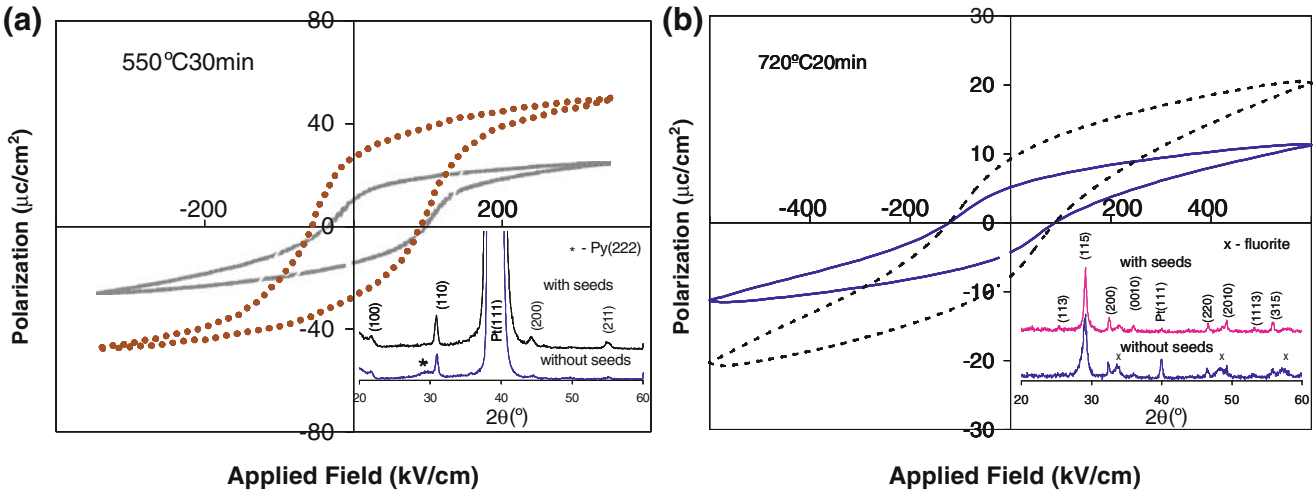

Fig. 1 Hysteresis loops of PZT (a) and SBT films (b) with and without seeds annealed at 550 °C/30 min and at 720 °C/20 min, respectively (*solid line*: unseeded; *dashed line*: seeded). *Inset* is the XRD patterns of the relative films

The SBT peaks are narrower in seeded films than unseeded ones, and the fluorite peaks are reduced. Literature reported that SBT films may be synthesized at temperatures ranging from 700 °C (when using Rapid Thermal Annealing) to 780–800 °C (when using conventional annealing) [5, 6, 8–11]. The presence of fluorite as an intermediate phase that can be converted to layered perovskite was commonly observed. This conversion was improved by the introduction of seeds. Previous studies on seeded SBT thin films reported that the use of seeds lowers the incubation time and temperature of the fluorite-to-Aurivillius phase transformation, while enhancing the transformation kinetics due to a decrease of the activation energy [5, 6].

The crystallization improvement in seeded films is reflected in their macroscopic electric response. Unseeded PZT films [Fig. 1(a)] have an average remanent polarization [(+Pr)+(−Pr)]/2 of about 12 μC/cm^2, while seeded PZT films exhibit an average remanent polarization of 23 μC/cm^2. The enhancement of the ferroelectric behavior as a consequence of the addition of nanometric seeds is also clearly observed in the hysteresis loops of SBT films [Fig. 1(b)]. The presence of seeds improves significantly the remanent polarization from 4.5 μC/cm^2 for unseeded to 8.2 μC/cm^2 for seeded SBT films, respectively. An increase of the remanent polarization value in both seeded PZT and SBT films were observed, reflecting the improved microstructure of seeded films.

The surface microstructure of these films is shown in Fig. 2. Although the root mean square (RMS) surface roughness calculated for seeded and unseeded PZT films, in 1.5×1.5 μm^2 frame, has the same 1.0 nm value, seeded PZT films [Fig. 2(a)] are characterized by a more uniform distribution of fine grain with an average size of 50 nm. Contrary, the surface morphology of unseeded PZT films [Fig. 2(b)] showed some bigger grains, not homogeneously distributed, and with a grain size ranging from 50 to 120 nm. Both seeded and unseeded SBT films [Fig. 2(c) and (d)] showed similar surface morphology with a nonuniform grain size distribution and grain size from 140 to 450 nm, being more obvious in unseeded films. The RMS roughness of seeded and unseeded SBT films calculated from a 1.5×1.5 μm^2 frame showed the same value of 10.7 nm. As in the situation of PZT films, seeded SBT films display a more homogeneous microstructure, while unseeded films showed a nonuniform microstructure with big grains surrounded by small grains. The presence of the nanoparticles and their action as heterogeneous nucleus sites seems to be the reason for the uniformity and small grain growth of seeded films.

The piezoresponse (domain) images of the PZT and SBT films are shown in insets of Fig. 2. Domains with opposite polarities will exhibit different contrast. Dark regions correspond to domains with polarization oriented towards the substrate, and bright regions correspond to domains with polarization terminated at the film surface. Grains with non-ferroelectric phase or polarization vector in-plane (or close to it) will exhibit intermediate gray contrast corresponding to vanishing piezoresponse. The piezoresponse images of seeded PZT films [inset of Fig. 2(a)] are characterized by strong domain contrast: deep bright and dark areas indicate significant out-of-plane component of polarization (circled by solid lines). At the same time, for unseeded PZT films [inset of Fig. 2(b)], a large fraction of gray regions (exhibiting weak piezoresponse signal) were observed. Seeded PZT films displayed higher percentage of well-defined domains than unseeded PZT films.

For SBT films, there exists a relative portion of grains with gray contrast indicating the presence of a non-ferroelectric phase or in-plane polarization. Considering the results from XRD, at this state, both seeded and unseeded

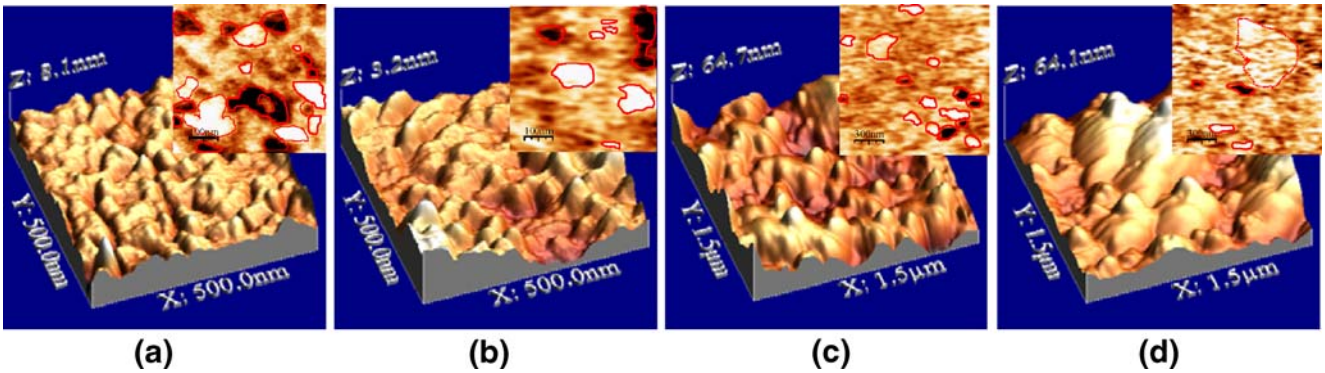

Fig. 2 AFM morphology images of PZT seeded (a), unseeded (b) and SBT seeded (c), and unseeded (d) films. *Insets* are corresponding local piezo-response images (*solid line circle*—well-defined domain region, *dashed line circle*—not well-defined, possible domain region)

films contain residual fluorite phase. However, the number of well-defined domains in seeded SBT films is higher than that in unseeded ones. Coherent with macroscopic XRD analysis, perovskite phase dominated seeded SBT films displaying stronger piezo-response signal than unseeded SBT film with higher amount of fluorite phase.

The local piezoloops were measured on individual grains, and the typical piezoloops of the films are shown in Fig. 3. In both cases, local piezoelectric d_{33} of seeded films show higher piezo-response signal than unseeded ones. It can be seen that in different material systems, seeded film always show a higher average remanent $d_{33}\left(\left(d_{33}^{+}-d_{33}^{-}\right)/2\right)$ coefficient value than that of unseeded films. This local electric characteristic is well consistent with the aforementioned macroscopic results. The macroscopic characteristic reflects the contribution of all local characteristics. Meanwhile, nonsymmetric piezoloops in the polarization direction were detected both in PZT and SBT films caused by self-polarization of the films [12–14]. Self-polarization occurs due to the presence of an internal electric field, which is at least as large as the coercive field at Curie temperature. Some authors suggested that this internal electric field is likely to be generated by oxygen vacancies at the bottom electrode/PZT film interface for the case of PZT films [12–14]. In seeded films, the interface between ferroelectric thin film and substrate was modified by the addition of seeds in the PZT precursor and substrate seeding in SBT films. Previous transmission electron microscopy (TEM) studies of PZT films [4] revealed that the meta-stable alloy Pt_xPb, observed in the interface between PZT and Pt electrode layer in early stage of annealing process, was suppressed in seeded films. Similarly, RBS studies of SBT films showed that a sharper interface between SBT films and platinum electrode is observed in seeded films when compared to their unseeded counterparts [15]. Unseeded SBT films displayed a stepped interface denoting some intermixing of Pt and film components. Such interface phenomena are suppressed in seeded ones. The change of the interface of PZT/bottom and SBT/bottom electrodes caused by the addition of seeds in PZT and SBT films consequently modifies the self-polarization state of the films, and seeded films showed less self-polarization level.

On the other hand, it is detected that the critical voltage (determined here, on a local level as V_{cr}, which is necessary to nucleate a new domain—Fig. 3) of seeded films is smaller than unseeded films in both PZT and SBT systems. Seeded films display a relatively easier nucleation of domain than unseeded films under the same applied field. The alignment of domains that occurs locally near the film–electrode interface is affected by the presence of seeds. The modification of interlayer state altered the final microscopic and macroscopic electric properties. The obstruction of the interdiffusion between films and the Pt layer by the seeds'

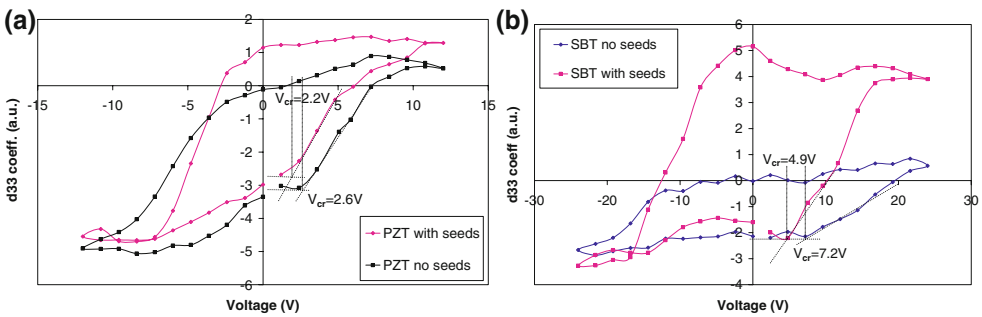

Fig. 3 Local piezoloops measured inside individual grains of PZT (a) and SBT (b) films with and without seeds (V_{cr}—critical voltage)

presence maintained the film composition within its stoichiometry. Superior electrical properties at a microscopic and macroscopic scale were revealed. This finding suggests that the thin film/Pt electrode interface is of great relevance for the ferroelectric behavior of PZT and SBT thin films.

4 Conclusions

The use of seeds in the CSD of PZT and SBT films contributes to lower the crystallization temperature of perovskite phase. Moreover seeds benefit from the thin film microstructure homogeneity (uniform grain size distribution and less interfacial reactions) and improve the ferroelectric properties. Higher remanent polarization values were obtained for both seeded PZT and SBT films than those unseeded ones at low annealing temperature (550 °C for PZT, 720 °C for SBT films). In both cases, local d_{33} coefficient of seeded film showed higher piezo-response signal than unseeded ones. Critical voltage of seeded films is smaller than that of unseeded ones, indicating an easier nucleation of domain under the same applied field. Recently, much attention has been paid to the ferroelectric film–electrode interface as a possible source for the degradation of electric properties. The application of seeds in ferroelectric films can be an alternative route to improve the interface sharpness, and hence, the electric response of thin films.

Acknowledgement The financial support from FCT and POCI/CTM/61071/2004 were acknowledged.

References

1. J.F. Scott, C.A. Paz de Araujo, Science **246**, 1400 (1989)
2. B.H. Park, B.S. Kang, S.D. Bu, T.W. Noh, J. Lee, W. Jo, Nature **401**(6754), 682 (1999)
3. A. Wu, I.M. Miranda Salvado, P.M. Vilarinho, J.L. Baptista, J. European Ceram. Soc. **17**, 1443 (1997)
4. A. Wu, P.M. Vilarinho, I. Reaney, I.M. Miranda Salvado, Chem. Mater. **15**, 1147 (2003)
5. Y.M. Sung, G.M. Anilkumar, S.J. Hwang, J. Mater. Res. **18**, 387 (2003)
6. G. González-Aguilar, M.E.V. Costa, Ferroelectrics **294**, 211 (2003)
7. A. Wu, P.M. Vilarinho, I.M. Reaney, I.M. Miranda Salvado, J.L. Baptista, Integ. Fer. **30**, 261 (2000)
8. T. Atsuki, N. Soyama, T. Yonezawa, K. Ogi, Jpn. J. Appl. Phys. **34**, 5096 (1995)
9. T.J. Boyle, C. Buchheit, M.A. Rodriguez, H.N. Al-Shareef, B. Hernandez, B. Scott, J.W. Ziller, J. Mater. Res. **11**, 2274 (1996)
10. K. Kato, C. Zheng, J.M. Finder, S.K. Dey, Y. Torii, J. Am. Ceram. Soc. **81**, 1869 (1998)
11. K. Anamuna, T. Hase, Y. Miyasaka, Appl. Phys Lett. **66**, 221 (1995)
12. G. Suchaneck, R. Koehler, P. Padmini, T. Sandner, J. Frey, G. Gerlach, Surf. Coat. Technol. **116**, 1238 (1999)
13. A.L. Kholkin, K.G. Brooks, D.V. Taylor, S. Hiboux, N. Setter, Integ. Fer. **22**, 525 (1998)
14. J. Frey, F. Schlenkrich, A. Schoenecker, Integ. Fer. **35**, 105 (2001)
15. G. González Aguilar, A. Wu, M.A. Reis, A.R. Ramos, I.M. Miranda Salvado, E. Alves, M.E.V. Costa, Surface Science **600**, 1780 (2006)